

RESEARCH

Open Access



GIN51 facilitates the development of lung adenocarcinoma via Wnt/ β -catenin activation

Luyuan Ma¹, Rongyang Li¹, Pengyong Li², Wenhao Yu¹, Zhanpeng Tang¹, Libo Si^{1*} and Hui Tian^{1*}

Abstract

Background Lung adenocarcinoma(LUAD) is the primary reason for cancer-related deaths globally. GINS1 has a significant regulatory function in DNA replication. It is overexpressed in various malignant tumors, but the specific molecular mechanisms of GINS1 in LUAD pathogenesis are not fully elucidated. This is the first report that GINS1 enhances LUAD by activating Wnt/ β -catenin signaling pathway, and may serve as a potential target for therapy.

Methods Bioinformatic analysis including analysis of difference, survival analysis and pathway enrichment, immunohistochemistry(IHC), western blotting(WB), and quantitative real time polymerase chain reaction(qRT-PCR) were used to detect GINS1 expression in LUAD cell lines and tissues. A range of in vivo and in vitro experiments, such as cck-8, EdU, cloning experiment, wound healing experiment and transwell experiment, confirmed that GINS1 facilitated the proliferation and migration of LUAD. Additionally, the potential mechanism of GINS1 was hypothesized through WB and transcriptome sequencing. The rescue experiment was used to verify our conclusion.

Results In this study, we discovered that GINS1 is significantly overexpressed in LUAD cell lines and tissues. Analysis of Kaplan – Meier survival data indicated that high levels of GINS1 expression are often linked to unfavorable survival outcomes. Additionally, a series of experiments showed that silencing GINS1 led to less proliferation and migration of LUAD cell lines, while its overexpression enhanced tumor progression. Furthermore, subcutaneous tumor experiments in nude mice supported the role of GINS1 in promoting tumor development in vivo. Lastly, transcriptome sequencing revealed that tumor progression is related to cell cycle (G1 to S phase transition associated with cyclinD) and β -catenin signaling pathway, which we subsequently validated using WB. A series of rescue experiment further confirmed that GINS1 facilitates the advancement of LUAD via the β -catenin signaling pathway.

Conclusions Our findings suggest that GINS1 plays a critical role in the progression of LUAD by modulating key molecular pathways, particularly the β -catenin signaling pathway, and it might serve as a potential new target of β -catenin signaling pathway for treatment of LUAD.

Keywords GINS1, Lung adenocarcinoma, Proliferation, Migration, B-catenin signaling pathway

*Correspondence:

Libo Si

silibo110@163.com

Hui Tian

tianhuiql@email.sdu.edu.cn

¹Department of Thoracic Surgery, Qilu Hospital of Shandong University, Jinan 250012, Shandong, China

²Department of Critical Care Medicine, Qilu Hospital of Shandong University, Jinan 250012, Shandong, China



© The Author(s) 2025. **Open Access** This article is licensed under a Creative Commons Attribution-NonCommercial-NoDerivatives 4.0 International License, which permits any non-commercial use, sharing, distribution and reproduction in any medium or format, as long as you give appropriate credit to the original author(s) and the source, provide a link to the Creative Commons licence, and indicate if you modified the licensed material. You do not have permission under this licence to share adapted material derived from this article or parts of it. The images or other third party material in this article are included in the article's Creative Commons licence, unless indicated otherwise in a credit line to the material. If material is not included in the article's Creative Commons licence and your intended use is not permitted by statutory regulation or exceeds the permitted use, you will need to obtain permission directly from the copyright holder. To view a copy of this licence, visit <http://creativecommons.org/licenses/by-nc-nd/4.0/>.

Introduction

Lung cancer ranks among the most prevalent cancers globally and is the leading cause of cancer-related deaths [1, 2]. Non-small cell lung cancer (NSCLC) is the most prevalent subtype, among them, lung adenocarcinoma (LUAD) is the most common, accounting for about 40% of all lung cancer patients [3, 4]. Due to the absence of clear symptoms in the initial stages of lung adenocarcinoma, most cases are identified at a more advanced stage. Consequently, the 5-year survival rate for patients is quite low, approximately 15% [5]. The current treatment methods of lung cancer primarily consisting of surgery, radiation therapy, chemotherapy, and molecular targeted therapies [6, 7]. Recently, the use of molecular targeted therapy and immunotherapy has expanded in lung cancer treatment, leading to notable improvements in patients' outcomes [8, 9]. Therefore, it is of great clinical importance for us to find new molecular targets for the treatment of lung cancer.

GIN51, also referred to as PSF1, forms a heterotetrameric GINS complex alongside GINS2, GINS3, and SLD5. These four subunits share similar protein sequences and spatial structures, creating a hollow, oval formation arranged in a clockwise manner [10, 11]. The GINS complex is crucial for growth and development, as it interacts with MCM through various subunits and CDC45. This collaboration results in the formation of the CDC45-MCM-GINS (CMG) complex, which stabilizes and enhances helicase activity, aids in the initiation of DNA replication, facilitates DNA bifurcation, and extends chromosome replication [12, 13]. Additionally, the GINS complex is significantly linked to the stability of biological genomes [14].

GIN51 is essential for early embryonic development, and a lack of GIN51 can result in developmental defects in embryos [15]. Additionally, research indicates that GIN51 can influence the cell cycle and cell proliferation by interacting with various receptors, growth factors, and other functional proteins [16]. Recent studies have highlighted GIN51's significant involvement in the advancement of malignant tumors [17]. Elevated GIN51 expression is frequently linked to unfavorable outcomes in several cancers, such as bladder cancer [18], colon cancer [19], liver cancer [20, 21], and glioblastoma [22, 23]. In diffuse large B-cell lymphoma (DLBCL), GIN51 can enhance tumor cell proliferation through the process of ubiquitination [24]. Furthermore, GIN51 may contribute to drug resistance in cancer cells [25, 26]. Nonetheless, the connection between GIN51 and lung adenocarcinoma has not been explored, and whether GIN51 enhances the progression of LUAD is exactly the question we wanted to investigate.

The Wnt signaling pathway is a very important signaling transduction pathway during the development of the

organism, especially playing a crucial role in the processes of embryonic development and cell differentiation [27]. The Wnt signaling pathway includes the classical Wnt/ β -catenin signaling pathway, the non-classical planar cell polarity pathway (PCP pathway), and the Wnt/ Ca^{2+} pathway [28]. The classical Wnt signaling pathway mainly functions by regulating the stability of the core factor β -catenin. When the signaling pathway is activated, Wnt ligands bind to the cell membrane receptors Frizzled and LRP5/6, inhibiting β -catenin binding to the degradation complex, gradually increasing the concentration of β -catenin in the cytoplasm and entering the nucleus to bind with the transcription factor TCF/LEF, activating the expression of downstream target genes, thereby affecting cell growth [29, 30]. It has been found that the abnormal activation of the Wnt/ β -catenin signaling pathway is closely related to the progression of various malignant tumors [31, 32].

In our study, we investigated the expression of GIN51 in LUAD, its biological function, and its possible mechanisms of action. Our findings revealed that GIN51 is significantly expressed in LUAD and facilitates tumor growth by influencing the β -catenin pathway. Consequently, GIN51 may serve as a novel molecular target for targeted therapy in LUAD.

Methods

Bioinformatic analysis and clinical samples

We used the GEPIA platform (<http://gepia2.cancer-pku.cn/>) to examine the expression of GIN51 across different malignant tumors and created a prognostic survival curve for GIN51 based on GEPIA and Kaplan-Meier survival analysis (<https://kmplot.com/analysis/>), all datasets used for analysis were obtained from The Cancer Genome Atlas (TCGA). The expression variations in lung adenocarcinoma data from TCGA were assessed using the Xiantao academic online database (<https://www.xiantaozi.com/>).

The LUAD tissue microarray (HLugA180Su08) was sourced from Shanghai Xinchao Biotechnology Company (SHYJS-CP-1904014), all patients provided written informed consent and remained anonymous. It comprises 98 LUAD tissue samples and 82 adjacent non-cancerous tissues, along with details on gender, age, clinical stage, and survival data for each patient. The study received approval from the Ethics Committee of Shanghai Xinchao Biotechnology Company.

Independent validation datasets were provided by the bioinformatics analysis platform used in the study. All analyses are performed with 95% confidence intervals, and the significance of p values is as follows: *, $P < 0.05$; **, $P < 0.01$; ***, $P < 0.001$; ****, $P < 0.0001$.

Cell culture and treatment

The BEAS-2B, H1299, A549, H1975 and PC9 LUAD cell lines were supplied by the Shanghai Cell Bank Research Center, which is part of the Chinese Academy of Sciences. After receiving the cells, we determined the cell lines through short tandem repeat analysis and examined every three months. The cell lines were respectively grown in TPMI-1640 Medium (Gibco)(H1299, H1975) and Dulbecco's Modified Eagle Medium (Gibco) (BEAS-2B, A549, PC9) in a humid 5% CO₂ incubator at 37°C. All mediums were supplemented with 10% fetal bovine serum (FBS; Gibco). During our experiment, we conducted an analysis of short tandem repeats for each cell line every 3 to 6 months, and we tested the cells for mycoplasma contamination using the MycoAlert Mycoplasma assay kit (Lonza) every 3 months. Small-interfering RNA (Suzhou Gemma Gene Co., LTD) and plasmid (Shandong Scientific Research Cloud Biotechnology Co. LTD) were transiently transfected in A549, PC9, and H1299 cell lines, respectively. The transfection was performed in accordance with the manufacturer's instructions using jetPRIME transfection reagent (Polyplus). The transfection system for each well consisted of 200 µl buffer, 4 µl transfection reagent and 5 µl Si-RNA or 2 µg plasmid. The cells were subsequently utilized for further experiments at approximately 48–72 h after transfection. The Sh-GINS1 lentiviruses were transfected into A549 cells (MOI:20), whereas the GINS1 overexpression lentiviruses were transfected in H1299 cells (MOI:10). Control transfection was performed for each lentivirus. The transfected cells were screened with purinomycin. All lentiviruses were purchased from Jikai Company. The small-interfering RNA and lentiviruses sequences are provided in Supplementary Table S1.

Western blotting

RIPA assay buffer (Beyotime) with 1% protease and phosphatase inhibitors was added into the cells and incubated on ice for 30 min to ensure complete lysis. The mixture was then centrifuged at 12,000 RPM at 4 °C for 15 min to collect the supernatant, which contained the protein sample. The protein concentration was determined using the BCA assay kit (Beyotime), with 15 µg of protein loaded per well. The proteins were separated using a 10% or 12% SDS-PAGE gel, followed by transfer to a polyvinylidene difluoride membrane. The membrane was treated with 5% skim milk at room temperature for 1 h, followed by an overnight incubation with primary antibodies on a shaking platform at 4 °C. The secondary antibody was then placed on a shaker and incubated for 1 h at room temperature prior to measuring luminescence. The target protein was identified using an enhanced chemiluminescence (ECL) after incubation of the second antibody. Proteins were normalized using GAPDH as

an internal control. The primary antibodies we use are shown in Supplementary Table S2.

Cell counting kit-8 cell proliferation assay

After transfection, cells for the treatment group and the control group were cultured in 96-well plates at a density of 2000 cells per well and allowed to incubate for 24, 48, 72, 96, and 120 h. The Cell Counting Kit-8 (CCK8; APEX BIO, #K1018) was added into the cells, after a two-hour incubation in the dark, the absorbance at 450 nm was recorded using an enzyme label. The experiment was conducted independently three times.

EdU assay

After transfection, cells for the treatment group and the control group were cultured in 96-well plates at a density of 20,000 cells per well and allowed to incubate overnight. EdU staining was conducted on the cells using an EdU In Vitro Kit (Beyotime), following the provided guidelines. Ultimately, images of the cells were captured using a fluorescent inverted microscope. The images were subsequently counted for statistics using ImageJ. The experiment was conducted independently three times.

Colony formation assay

After transfection, cells for the treatment group and the control group were cultured in 6-well plates at a density of 1000 cells per well and the culture was terminated when most of the cell colonies in the well plates had proliferated to more than 50 cells. The cells were then fixed using 4% paraformaldehyde for 25 min and subsequently stained with 0.5% crystal violet for another 25 min. Rinse with phosphate buffered saline (PBS) up to three times, let it dry and take pictures with the camera. The images were subsequently counted for statistics using ImageJ. The experiment was conducted independently three times.

Wound-healing assay

After transfection, cells for the treatment group and the control group were cultured in a six-well plate until the cells were almost completely confluent. A 200 µl pipette tip was used to create a vertical line on the plate, ensuring that the line was straight and of consistent width. After rinsing the area three times with PBS, the cells were incubated in serum-free medium rather than medium containing serum. The width of the scratches was captured using a microscope at 0 h and 24 h respectively. The experiment was conducted independently three times.

Transwell assay

Cells for the treatment group and the control group were added in the transwell upper chamber containing serum-free medium, while 700 µl of medium with 20% FBS was

added to the transwell lower chamber. After incubating at 37 °C for 24 h, the cells in the upper chamber were lightly scrubbed using a cotton swab. The cells were then fixed with 4% paraformaldehyde for 25 min, stained with 0.5% crystal violet for another 25 min, and finally observed under a microscope for photography. The experiment was conducted independently three times.

Flow cytometry

The cells were grown in six-well plates, and after 48 h, cell cycle assays were conducted using flow cytometry. The Cell Cycle Kit (Multi Sciences) was utilized to analyze the cell cycle following the manufacturer's guidelines. The cell cycle of the samples was detected by flow cytometry. Flowjo was used to analyze the test results.

In vivo experiments

Knockdown and overexpression lentiviruses were transfected in cell lines A549 and H1299, respectively. Four-week-old nude mice were provided by Huafukang company. The nude mice were assigned numbers based on their weight, ranging from 1 to 20, and categorized into five groups. Each of these groups was then randomly split into four subgroups using a random number table. The living environment of the mice was identical. The mice in the four cages were injected separately in the armpits with A549 Sh-NC, A549 Sh-GINS1, H1299 Vector, and H1299 oe-GINS1 to create subcutaneous tumor models, and tumor sizes were recorded every week by the vernier caliper, tumor volume was calculated as $(\text{long diameter} \times \text{short meridian}^2)/2$. After 35 days, ensure that the nude mice are growing well and no cachexia has occurred, the mice were euthanized by CO₂ asphyxia, and the tumors were collected and weighed. Photographs of the mice and tumors were taken. We performed immunohistochemical staining of tumor tissues from nude mice for H&E and Ki67 (GB121141-100, 1:300). Sevier Corporation supplied the tumor immunochemical staining for the nude mice. The experiment was approved and monitored by the Medical Ethics Committee of Qilu Hospital of Shandong University. (DWLL-2024-029)

Data processing and transcriptome sequencing

Data on GINS1 expression was sourced from The Cancer Genome Atlas (TCGA) (<https://tcga-data.nci.nih.gov/tcga/>) databases. Transcriptome sequencing was conducted by LC Biotechnology Company. The mRNA transcripts were identified through transcriptome sequencing, revealing differences in expression between GINS1 knockdown A549 cells and control A549 cells. FastQC (v0.12.1) was used for quality control of raw sequencing data, and STAR aligner (v2.7.10a) was used for genome alignment. Gene quantification was performed with featureCounts (v2.0.3), differential expression analysis was

done with DESeq2 (v1.34.0), and correction for multiple testing was performed with the Benjamini-Hochberg method. Data were analyzed using the $2^{-\Delta\Delta C_t}$ method, and statistical significance was assessed by paired t-test ($P < 0.05$). Kyoto Encyclopedia of Genes and Genomes (KEGG) pathway enrichment analysis was performed on transcriptome sequencing data to screen out the signaling pathways and molecular proteins related to GINS1 promoting the progression of lung adenocarcinoma. The KEGG pathway enrichment diagram was created using the cloud platform offered by the company. (<https://www.omicstudio.cn>).

B-catenin inhibitors

Obtain specific β -catenin inhibitor MSAB (YEASEN), dissolve with dimethyl sulfoxide (DMSO) and store in a -80 °C refrigerator. H1299 cells were categorized into four groups: oe-NC + DMSO, oe-GINS1 + DMSO, MSAB, and oe-GINS1 + MSAB. After transfecting with the overexpression plasmid for 24 h, inhibitors and an equal volume of DMSO were introduced, and subsequent experiments were performed after an additional 24 h of incubation.

Statistical analysis

All experimental data were analyzed with GraphPad Prism Software, and the findings were presented as the mean \pm standard deviation. (SD). Data were assessed for normality using the Shapiro-Wilk test prior to analysis of parameters. Our experiments were all adjusted for multiple testing. The difference between the two data sets was assessed using a two-tailed T-test. A one-way analysis of variance (ANOVA) was performed to evaluate the differences among several groups. Multiple testing correction was performed using the Bonferroni method to ensure that the probability of making an error was within 5%. Additionally, the Kaplan-Meier survival analysis, Pearson Chi-squared test, and Fisher exact test were utilized as appropriate. A P-value below 0.05 was considered statistically significant.

Results

GINS1 is significantly expressed in LUAD and is linked to a negative prognosis

To investigate the role of GINS1 in LUAD, firstly, we found that GINS1 expression was significantly elevated in LUAD in relation to normal tissues by analyzing data from GEPIA platform (<http://gepia2.cancer-pku.cn/>) and the TCGA databases (Fig. 1A and B). We then assessed the correlation between GINS1 expression and patient prognosis in LUAD using the GEPIA platform and Kaplan-Meier survival analysis (<https://kmplo.t.com/analysis/>), which indicated that patients with high GINS1 levels had a worse prognosis (Fig. 1C). All analyses are performed with 95% confidence intervals, and the

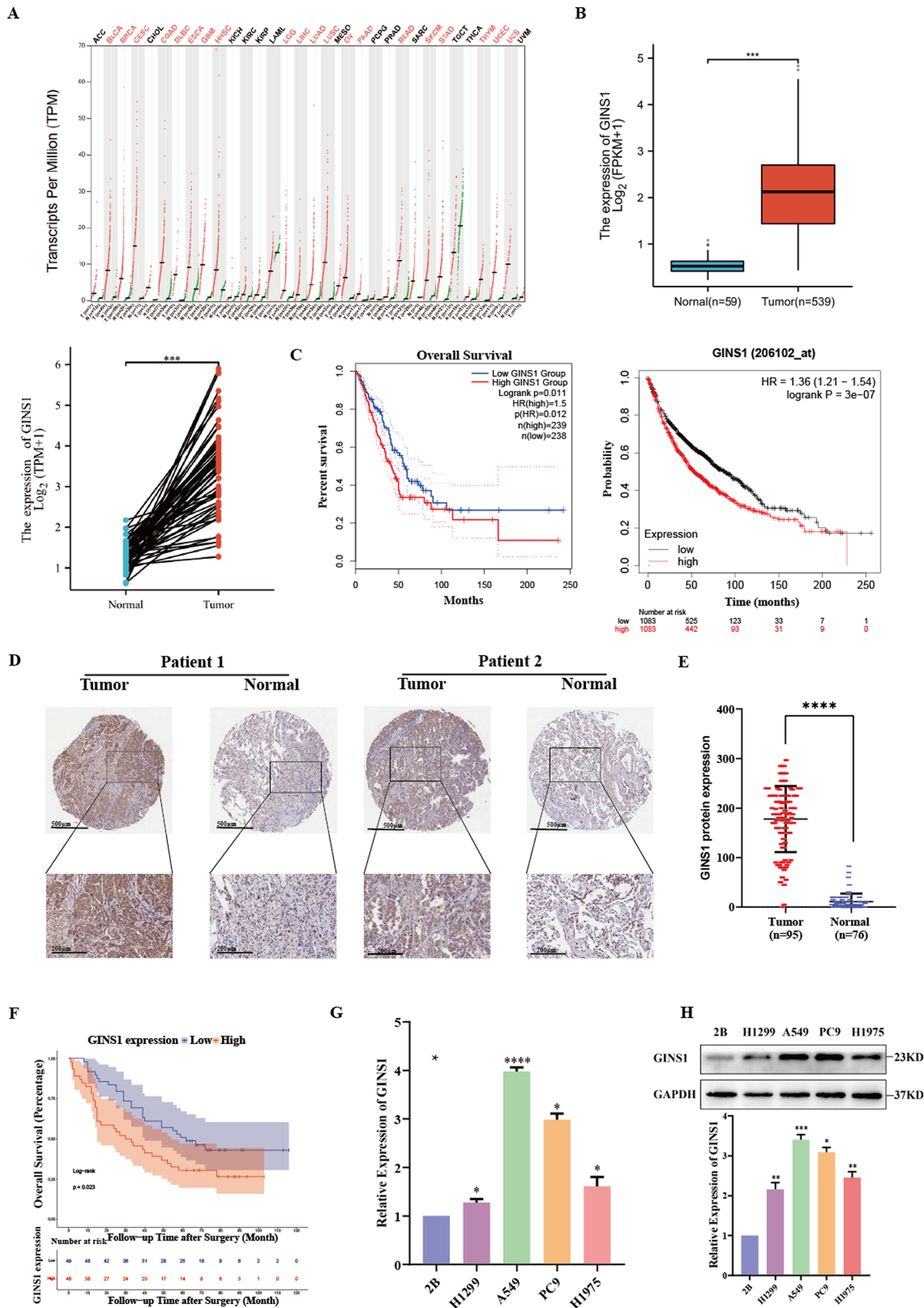


Fig. 1 (See legend on next page.)

(See figure on previous page.)

Fig. 1 GINS1 is highly expressed in lung adenocarcinoma tissues and is linked to poor prognosis of patients. **(A)** Relationship between GINS1 expression in various cancers and normal tissues. **(B)** The expression of GINS1 in LUAD and adjacent normal tissues according to TCGA database. **(C)** GEPIA website and K-M online website were used for overall survival analysis of GINS1 high expression and low expression and the prognosis of the disease. **(D)** IHC images of representative tissue microarrays showing the difference in GINS1 expression between lung adenocarcinoma and adjacent normal tissues. Scale bar, 500 μm (upper), 200 μm (down). **(E)** IHC score for GINS1 in the tissue microarray. **(F)** The K-M survival analysis of lung adenocarcinoma patients was performed according to tissue microarray. **(G, H)** Expression of GINS1 at mRNA and protein levels in five lung adenocarcinoma cell lines. *, $P < 0.05$; **, $P < 0.01$; ***, $P < 0.001$; ****, $P < 0.0001$. LUAD: lung adenocarcinoma; IHC: immunohistochemistry; TCGA: The Cancer Genome Atlas

significance of p values is as follows: *, $P < 0.05$; **, $P < 0.01$; ***, $P < 0.001$; ****, $P < 0.0001$. Subsequently, we conducted immunohistochemical analysis on tissue microarrays from 98 LUAD samples, it was independently evaluated by two senior pathologists who were blinded to clinicopathological parameters and patient prognostic information. The H-score system was used for scoring, and immunohistochemical scores showed that GINS1 expression in LUAD tissues was significantly higher than that in corresponding adjacent normal lung tissues. The Kaplan-Meier survival analysis of these 98 samples further confirmed that elevated GINS1 expression was associated with poor prognosis (Fig. 1D, E and F). Finally, we used WB and qRT-PCR to detect the expression of GINS1 in four LUAD cell lines (H1299, A549, H1975, PC9) and BEAS-2B in normal lung epithelial cells, and the findings indicated that the level of GINS1 expression in LUAD cell lines was greater compared to that in normal lung epithelial cells (Fig. 1G and H).

GINS1 promoted the proliferation and migration of LUAD cells in vitro

Using WB and qRT-PCR, we observed that among the four LUAD cell lines, GINS1 expression was highest in A549 and PC9 cells, while it was lowest in H1299 cells. Consequently, we chose two small-interfering RNA sequences to reduce GINS1 expression in A549 and PC9 cells, and we used an overexpression plasmid to increase GINS1 levels in H1299 cells. The effectiveness of the knockdown and overexpression was confirmed through WB and qRT-PCR (Supplementary Fig. 1A, 1B, 1C), after which we proceeded with further experiments. We used CCK-8, EdU, and colony formation assays to assess the proliferation capabilities of the treated cells. Compared to the control group, we found a significant reduction in the proliferation of tumor cells following GINS1 knockdown, while GINS1 overexpression led to a notable increase in tumor cell proliferation compared to the control group (Fig. 2A, B and C). To evaluate the migration abilities of the treated cells, we conducted transwell and wound-healing assays. Compared to the control group, our analysis revealed that the number of migrating tumor cells and the wound healing area decreased after GINS1 knockdown, whereas both metrics increased following GINS1 overexpression (Fig. 2D). Based on these findings, we determined that GINS1 plays a role in promoting the proliferation and migration of LUAD cells.

GINS1 promotes the proliferation of LUAD cells in vivo

To further investigate the impact of GINS1 on tumor growth, we conducted an in vivo experiment. We created a lentivirus by choosing the small-interfering RNA sequence that demonstrated the highest knockdown efficiency, leading to the establishment of stable A549 knockdown cell lines and H1299 overexpressing cell lines. The effectiveness of these modifications was confirmed through WB and qRT-PCR (Supplementary Fig. 1D). Subsequently, we injected the modified cells into the armpits of BALB/c-nude mice to create a subcutaneous tumor model. The findings indicated that, in comparison to the control group, the knockdown of the GINS1 gene significantly decreased the tumor growth rate, tumor volume, and tumor weight (Fig. 3A). Conversely, the GINS1 overexpression group exhibited the opposite effect (Fig. 3B). Our findings were additionally validated by immunohistochemical analyses (Fig. 3C and D), the expression level of Ki-67 in Sh-GINS1 group was significantly lower than that in the control group, while the expression level of Ki67 in oe-GINS1 group was significantly higher than that in the control group. These results suggest that GINS1 enhances the proliferation of LUAD cells in vivo.

GINS1 affects the progression of LUAD cells by activating the β -catenin signaling pathway

While a series of functional tests have indicated that GINS1 can facilitate the progression of LUAD, the specific mechanism behind its action remains unclear. To investigate the role of GINS1 in the progression of LUAD, we conducted transcriptome sequencing following the knockdown of GINS1 in A549 cells. Notably, Kyoto Encyclopedia of Genes and Genomes (KEGG) pathway enrichment analysis indicated that GINS1 expression influences the Wnt signaling pathway (Fig. 4A), and previous studies have suggested that GINS1 can interact with β -catenin to promote tumor growth (Fig. 4B). Consequently, we used WB to assess the expression of proteins linked to the β -catenin signaling pathways. The results demonstrated a positive correlation between GINS1 and the protein expression within this signaling pathway, then we examined the downstream related proteins: EMT and cell cycle (Fig. 4C, D and E). The impact of GINS1 on the cell cycle was additionally validated using flow cytometry (Fig. 4F, G and H). Based on this, we illustrated the role of

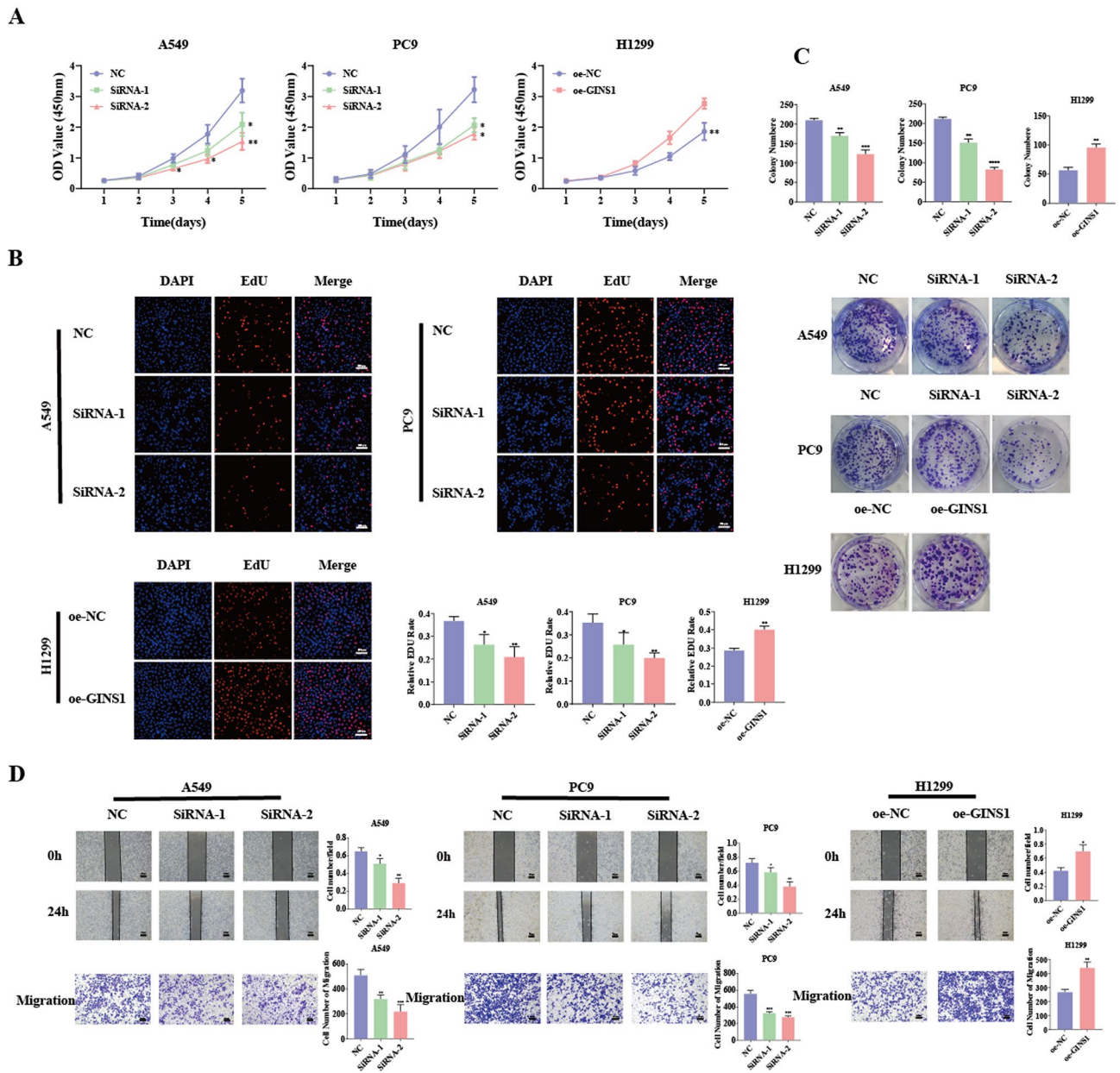


Fig. 2 GINS1 promoted the proliferation and migration of LUAD cells in vitro. A-C, CCK-8 (A), EdU assay (B), and colony formation assay (C) were employed to assess alterations in cell proliferation following GINS1 knockdown in A549 and PC9 cells, as well as GINS1 overexpression in H1299 cells. Scale bar of EdU assay, 100 μ m. (D) The migration capability of A549, PC9, and H1299 cells following GINS1 knockdown and overexpression was assessed using wound healing and transwell migration assays. Scale bar of wound healing, 200 μ m. Scale bar of transwell migration assays, 200 μ m. *, $P < 0.05$; **, $P < 0.01$; ***, $P < 0.001$; ****, $P < 0.0001$. LUAD: lung adenocarcinoma; CCK8: cell counting kit-8; EdU: 5-ethynyl-2-deoxyuridine

GINS1 in this signaling pathway and explained the mechanism of GINS1 in promoting cancer.

Rescue experiments

To further illustrate that GINS1 enhances the progression of LUAD by activating the β -catenin signaling pathways, Co-immunoprecipitation (Co-IP) assays, both endogenous and exogenous, were conducted to confirm if GINS1 and β -catenin interact with one another to carry

out their functions (Fig. 5A and B). Then we used a specific inhibitor MSAB to inhibit β -catenin expression in H1299 cells. The results of WB showed that MSAB could specifically inhibit the expression of β -catenin and its associated proteins, which could be reversed by overexpression of GINS1 (Fig. 5C). We then conducted a series of functional assays to validate this observation. The results revealed that MSAB decreased the proliferation and migration of LUAD, and this effect was reversible

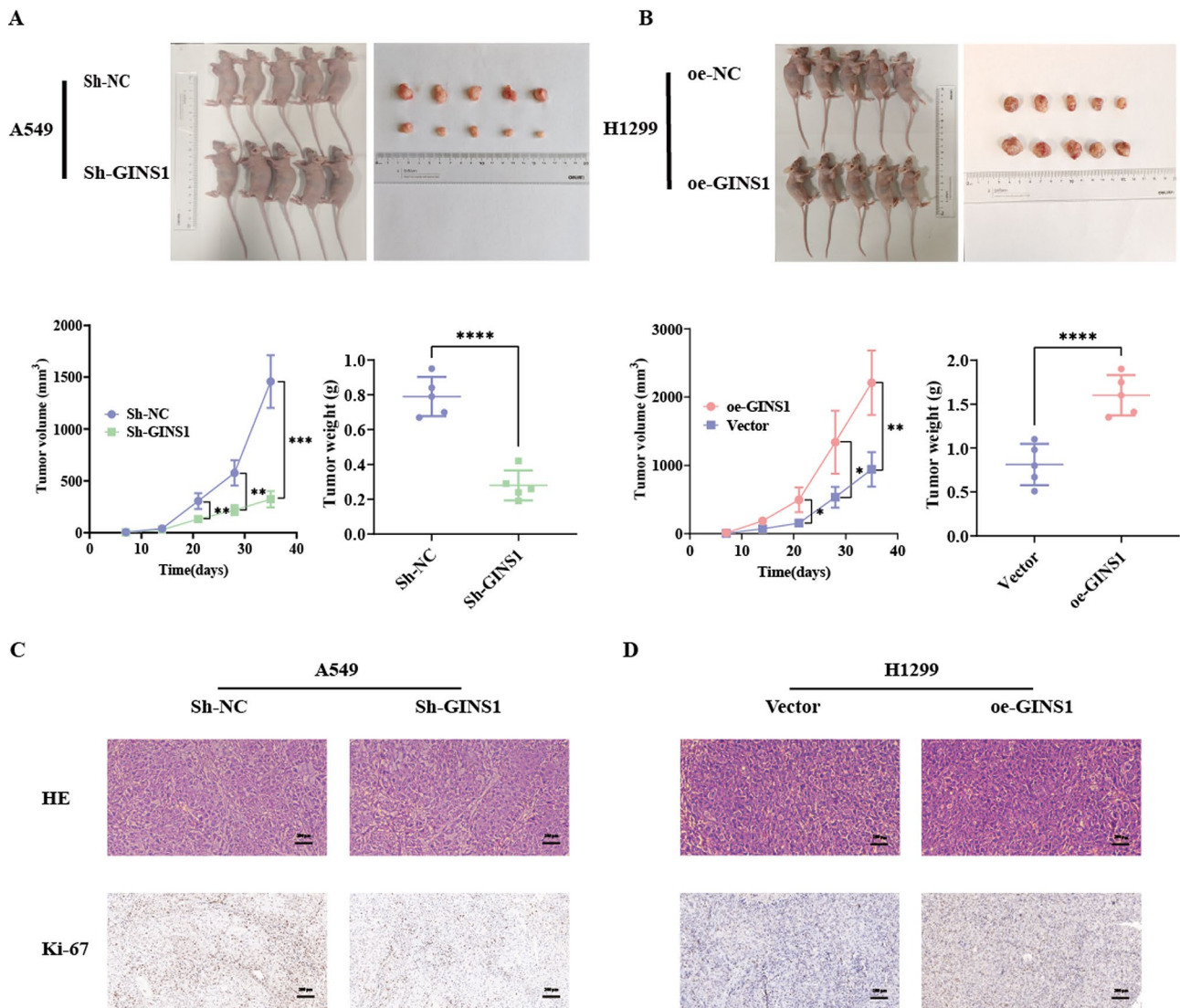


Fig. 3 GINS1 promotes the proliferation of LUAD cells in vivo. (A, B) Pictures of tumors of mice, growth curves of tumors, and weights of tumors in knock-down and overexpression groups. (C, D) Representative HE and IHC images from different groups of tumors. Scale bar, 200 μ m. *, $P < 0.05$; **, $P < 0.01$; ***, $P < 0.001$; ****, $P < 0.0001$. LUAD: lung adenocarcinoma; IHC: immunohistochemistry; HE: hematoxylin-eosin

with the overexpression of GINS1 (Fig. 5D, E, F and G). This strongly confirmed that GINS1 facilitates the progression of LUAD by modulating the β -catenin signaling pathway.

Discussion

This research revealed that GINS1 is highly expressed in LUAD tissues, and elevated levels of GINS1 are frequently linked to unfavorable outcomes for patients. Additionally, it was shown for the first time that GINS1 facilitate the advancement of LUAD by activating the Wnt/ β -catenin signaling pathway. Overall, the findings indicate that GINS1 could serve as a promising molecular target for guiding clinical treatment of LUAD.

GINS1 is a key part of the heterotetrameric GINS complex, which is essential for the CMG helicase involved in starting DNA replication and advancing DNA replication forks. Research has shown that GINS1 contributes to tumor growth in various cancers, including bladder, stomach, liver, glioblastoma, and lymphoma, and is associated with unfavorable outcomes for patients.

The Wnt/ β -catenin signaling pathway is crucial in the development of tumors [33–35]. Wnt/ β -catenin is the prototypical Wnt signaling pathway. Once secreted, it can bind to particular receptors on the cell membrane, influencing the accumulation or breakdown of β -catenin through the phosphorylation and dephosphorylation of various downstream proteins. When this pathway is abnormally activated, it can disrupt various normal

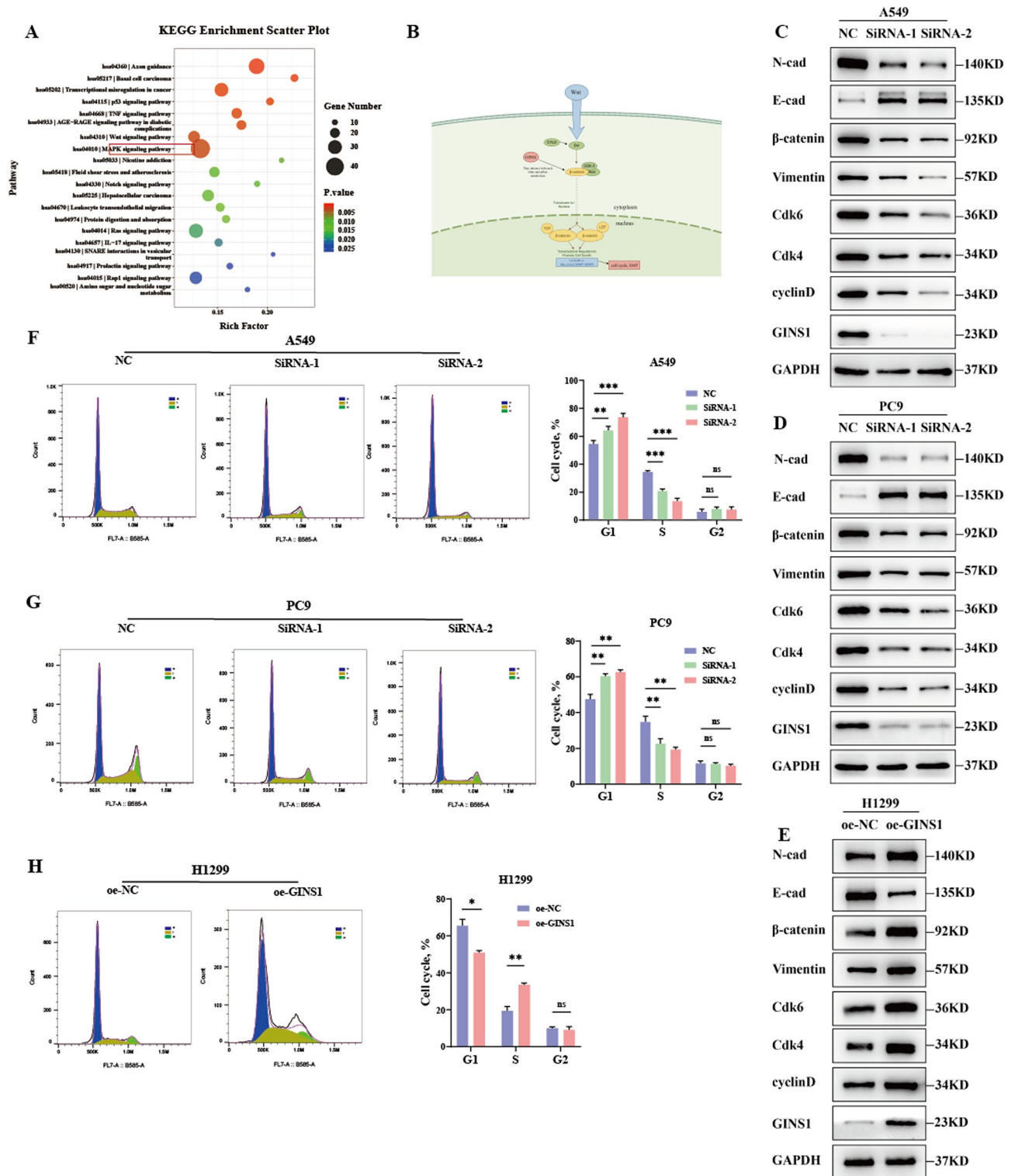


Fig. 4 GINS1 affects the progression of LUAD cells by activating the β -catenin signaling pathway. **(A)** KEGG pathway enrichment analysis of the transcriptome sequencing data. **(B)** Schematic representation of the mechanism of GINS1 and wnt pathway by Figdraw. **(C-E)** The expression of Wnt/ β -catenin pathway related proteins was detected by WB. **(F-H)** Cell cycle detection by flow cytometry after GINS1 was knocked down in A549 and PC9 cells, and after GINS1 was overexpressed in H1299 cells. *, $P < 0.05$; **, $P < 0.01$; ***, $P < 0.001$; ****, $P < 0.0001$. LUAD: lung adenocarcinoma; KEGG: Kyoto Encyclopedia of Genes and Genomes

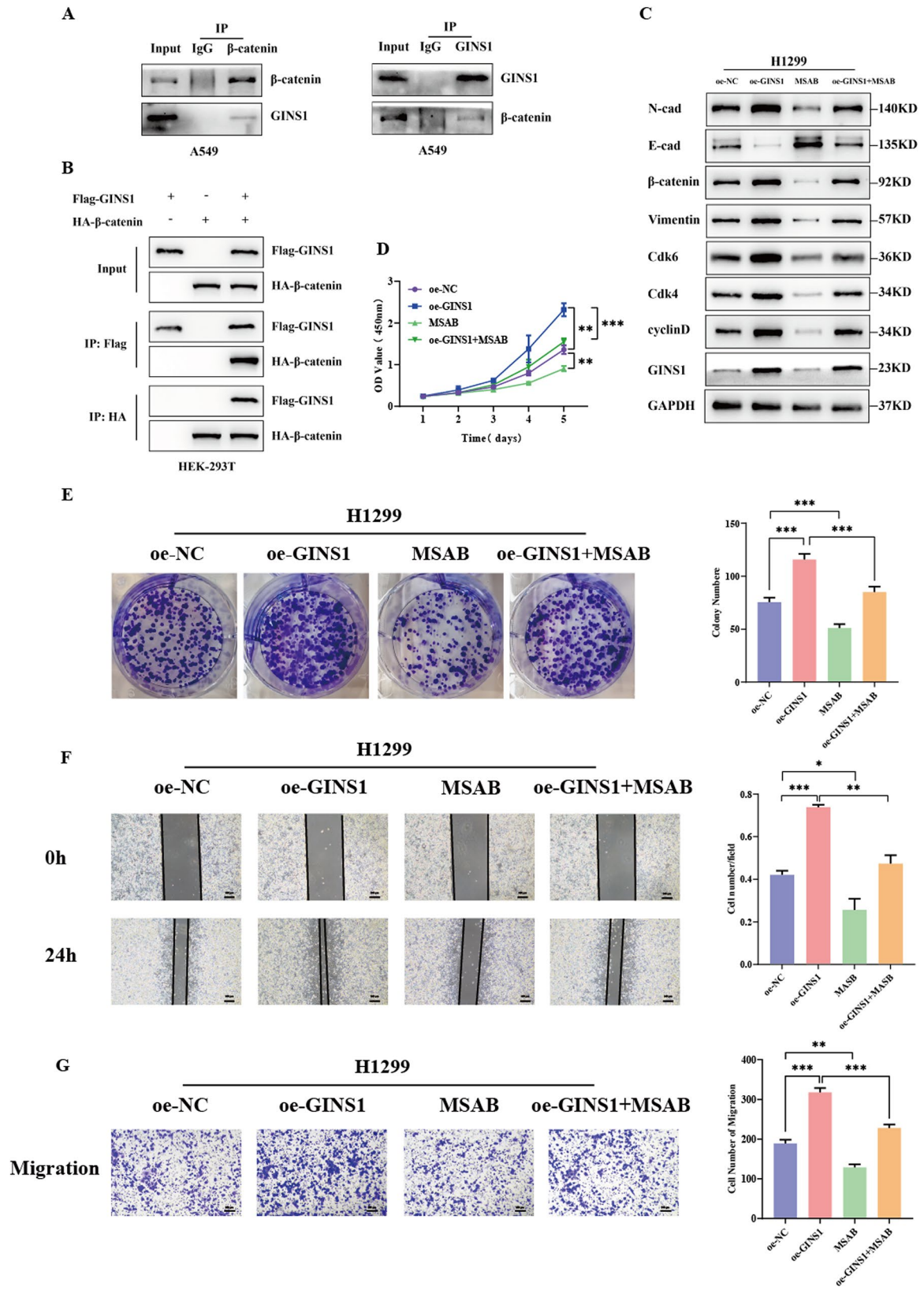


Fig. 5 (See legend on next page.)

(See figure on previous page.)

Fig. 5 GINS1 further regulates Wnt signaling by affecting β -catenin. **(A, B)** Endogenous and exogenous Co-IP confirmed that GINS1 could interact with β -catenin. **(C)** H1299 cells that overexpress GINS1 were treated for 24 h with the specific inhibitor MSAB or an equivalent volume of DMSO, and the associated signaling pathways were analyzed using WB. **(D-G)** CCK-8 **(D)**, colony formation assay (E), wound healing **(F)** and transwell migration assays **(F)** were conducted using H1299 cells that overexpress GINS1, which were treated for 24 h with the specific inhibitor MSAB or an equal volume of DMSO. *, $P < 0.05$; **, $P < 0.01$; ***, $P < 0.001$; ****, $P < 0.0001$. Co-IP: Co-immunoprecipitation; DMSO: dimethyl sulfoxide; WB: western blotting; CCK-8: cell counting kit-8

bodily functions, including cell growth and embryonic development, leading to the formation and spread of tumors [28, 33]. Research indicates that around 50% of malignant tumors, including LUAD, exhibit abnormal activation of the Wnt/ β -catenin signaling pathway [36]. Targeting the Wnt/ β -catenin pathway has been used to treat a variety of cancers [37, 38]. EMT and CyclinD1 are typical regulatory pathways of the Wnt/ β -catenin signaling pathway [39–41]. EMT is closely related to the invasion and migration ability of tumor cells. Our experiments showed that high levels of GINS1 enhance the migration of LUAD cells, leading us to associate this effect with the abnormal activation of EMT. Consequently, we examined the expression of EMT-related proteins E-cadherin, N-cadherin, and Vimentin in LUAD cells with both GINS1 knockdown and overexpression, and the findings aligned with our expectations. We conclude that GINS1 facilitates the migration of LUAD via the Wnt/ β -catenin/EMT pathway. CyclinD1 plays a crucial role in the cell cycle. It is the first to change in response to external growth factors or internal regulatory signals, facilitating the transition from the G1 to S phase, and is involved in DNA replication and repair. Additionally, it triggers the phosphorylation of histone H1 kinase and regulates cell proliferation, differentiation, and apoptosis [42–45]. We detected the expression of Cyclin D1 and its downstream factors cdk4 and cdk6 in treated cells [46], and found that they were positively correlated with the expression of GINS1. To further validate our hypothesis, we conducted cell cycle experiments, which confirmed that GINS1 enhances tumor proliferation via the Wnt/ β -catenin/CyclinD1 signaling pathway.

β -catenin plays an essential role in the Wnt/ β -catenin signaling pathway. β -catenin is synthesized in the cytoplasm, and when activated by upstream signals, it is transported from the cytoplasm to the nucleus to interact with downstream factors TCF/LEF [32, 47]. This interaction leads to the activation of various target genes (including c-Jun, Cyclin D1, and c-Myc), which then carry out different biological functions [31]. Aberrant accumulation of β -catenin is critical for tumor progression. In thyroid cancer, KDM1A reduces the levels of two key Wnt inhibitors, APC2 and DKK1, by demethylating h3k4me1/2 in the promoter region of APC2 and the non-histone protein HIF-1a. An increase in β -catenin levels accelerates the progression of thyroid cancer [38]. In breast cancer, Bruceine D can prevent the formation of the Trop2/ β -catenin complex, enhance the degradation

of β -catenin, and hinder the progression of breast cancer. Thus, specifically targeting the regulation of β -catenin is highly important for cancer treatment [48]. β -catenin tends to accumulate abnormally in tumor cells, which may be related to the abnormal function of phosphorylation-dependent Axin complex. This complex is made up of the scaffold protein Axin, the tumor-suppressing product of the adenomatous polyposis coli (APC) gene, casein kinase 1 (CK1), and glycogen synthase kinase 3 (GSK3). GSK3 serves a crucial regulatory function within the complex by phosphorylating the amino terminal region of β -catenin [49–51]. This modification leads to β -catenin being targeted by E3 ubiquitin ligase, resulting in its ubiquitination and subsequent degradation by the proteasome. This insight is significant for our investigation into how GINS1 influences the Wnt/ β -catenin signaling pathway. Additionally, we found that GINS1 directly interact with β -catenin, enhancing its expression and facilitating its transport into the nucleus, some articles also suggest a similar process [20]. However, the precise way it works is still not understood.

In the end, it needs to be further examined whether GINS1 directly interacts with β -catenin to induce changes in phosphorylation or if it prevents the degradation of β -catenin through ubiquitin phosphorylation. How can these findings be effectively applied to animal models or clinical studies? Is GINS1 a promising target for drug development in the treatment of LUAD? Whether GINS1 affects LUAD progression through other mechanisms? These are all questions that we will have to seriously explore in the future.

Conclusion

In summary, GINS1 plays an important role in tumor progression. Our study demonstrated that GINS1 promotes the progression of LUAD and is closely associated with poor prognosis. This study clarifies the tumor-promoting role of GINS1, which accelerates the cell cycle and EMT in tumor cells by activating the Wnt/ β -catenin signaling pathway, but the specific mechanism still needs to be further explored. Our results suggest that GINS1 has important medical significance in the diagnosis and treatment of LUAD, and GINS1 holds potential as a therapeutic target, though further studies are required to validate its clinical applicability. However, our article also has certain limitations. More experiments are needed to verify the specific mechanism of GINS1 and its potential as a molecular target.

Abbreviations

LUAD	Lung adenocarcinoma
IHC	Immunohistochemistry
HE	Hematoxylin-eosin
WB	Western blotting
qRT-PCR	Quantitative real time polymerase chain reaction
NSCLC	Non-small cell lung cancer
CMG	CDC45-MCM-GINS
DLBCL	Diffuse large B-cell lymphoma
FBS	Fetal bovine serum
MOI	Multiplicity of infection
SDS-PAGE	Sodium dodecyl sulfate - polyacrylamide gel electrophoresis
ECL	Enhanced chemiluminescence
CCK-8	Cell counting kit-8
EdU	5-ethynyl-2-deoxyuridine
PBS	Phosphate buffered saline
TCGA	The Cancer Genome Atlas
KEGG	Kyoto Encyclopedia of Genes and Genomes
DMSO	Dimethyl sulfoxide
ANOVA	A one-way analysis of variance
SD	Standard deviation
Co-IP	Co-immunoprecipitation
EMT	Epithelial-mesenchymal transition
APC	Adenomatous polyposis coli
CK1	Casein kinase 1
GSK3	Glycogen synthase kinase 3

Supplementary Information

The online version contains supplementary material available at <https://doi.org/10.1186/s12957-025-03786-2>.

Supplementary Material 1: **Supplementary Fig. 1.** Verification of the efficiency of cell treatment. (A-C) The effectiveness of the knockdown in A549 and PC9 and overexpression in H1299 was confirmed through WB and qRT-PCR. (D) The efficiency of silenced and overexpressed lentiviruses in A549 and H1299 was verified by WB and qRT-PCR. *, $P < 0.05$; **, $P < 0.01$; ***, $P < 0.001$; ****, $P < 0.0001$. WB: western blotting; qRT-PCR: quantitative real time polymerase chain reaction

Supplementary Material 2

Supplementary Material 3

Supplementary Material 4

Acknowledgements

Not applicable.

Author contributions

ML, SL and TH give the conception and design, ML finished most of the experiments, LP and TZ helped to complete some experiments, LR and YW provided the experimental guidance and help. All authors read and approved the final manuscript.

Funding

This study was funded by Taishan Scholar Program of Shandong Province (ts201712087), General Program of National Natural Science Foundation of China (82472814).

Data availability

All data are generated from public data, which has been shown in the article. The data that support the findings of this study are available on request from the corresponding author.

Declarations**Ethics approval and consent to participate**

Human experimental ethics were supplied by Shanghai Xinchao Biotechnology Company (SHYJS-CP-1904014), while Qilu Hospital of

Shandong University provided the ethics for experimental animals (DWLL-2024-029).

Consent for publication

Not applicable.

Competing interests

The authors declare no competing interests.

Received: 24 November 2024 / Accepted: 29 March 2025

Published online: 07 April 2025

References

1. Siegel RL, Miller KD, Wagle NS, Jemal A. Cancer statistics, 2023. *CA Cancer J Clin.* 2023;73(1):17–48.
2. Sung H, Ferlay J, Siegel RL, Laversanne M, Soerjomataram I, Jemal A, et al. Global cancer statistics 2020: GLOBOCAN estimates of incidence and mortality worldwide for 36 cancers in 185 countries. *CA Cancer J Clin.* 2021;71(3):209–49.
3. Nicholson AG, Tsao MS, Beasley MB, Borczuk AC, Brambilla E, Cooper WA, et al. The 2021 WHO classification of lung tumors: impact of advances since 2015. *J Thorac Oncol.* 2022;17(3):362–87.
4. Herbst RS, Morgensztern D, Boshoff C. The biology and management of non-small cell lung cancer. *Nature.* 2018;553(7689):446–54.
5. Reck M, Rabe KF. Precision diagnosis and treatment for advanced Non-Small-Cell lung cancer. *N Engl J Med.* 2017;377(9):849–61.
6. Molina JR, Yang P, Cassivi SD, Schild SE, Adjei AA. Non-small cell lung cancer: epidemiology, risk factors, treatment, and survivorship. *Mayo Clin Proc.* 2008;83(5):584–94.
7. Tran TO, Vo TH, Le NQK. Omics-based deep learning approaches for lung cancer decision-making and therapeutics development. *Brief Funct Genomics.* 2024;23(3):181–92.
8. Tran TO, Lam LHT, Le NQK. Hyper-methylation of ABCG1 as an epigenetics biomarker in non-small cell lung cancer. *Funct Integr Genomics.* 2023;23(3):256.
9. Li Y, Wu X, Yang P, Jiang G, Luo Y. Machine learning for lung cancer diagnosis, treatment, and prognosis. *Genomics Proteom Bioinf.* 2022;20(5):850–66.
10. Choi JM, Lim HS, Kim JJ, Song OK, Cho Y. Crystal structure of the human GINS complex. *Genes Dev.* 2007;21(11):1316–21.
11. Takayama Y, Kamimura Y, Okawa M, Muramatsu S, Sugino A, Araki H. GINS, a novel multiprotein complex required for chromosomal DNA replication in budding yeast. *Genes Dev.* 2003;17(9):1153–65.
12. Kubota Y, Takase Y, Komori Y, Hashimoto Y, Arata T, Kamimura Y, et al. A novel ring-like complex of xenopus proteins essential for the initiation of DNA replication. *Genes Dev.* 2003;17(9):1141–52.
13. Geng Y, Chen S, Yang Y, Miao H, Li X, Li G, et al. Long-term exposure to genistein inhibits the proliferation of gallbladder cancer by downregulating the MCM complex. *Sci Bull (Beijing).* 2022;67(8):813–24.
14. Xia Y, Sonnevile R, Jenkyn-Bedford M, Ji L, Alabert C, Hong Y, et al. DNSN-1 recruits GINS for CMG helicase assembly during DNA replication initiation in *Caenorhabditis elegans*. *Science.* 2023;381(6664):ead4932.
15. Ueno M, Itoh M, Kong L, Sugihara K, Asano M, Takakura N. PSF1 is essential for early embryogenesis in mice. *Mol Cell Biol.* 2005;25(23):10528–32.
16. Cottineau J, Kottemann MC, Lach FP, Kang YH, Vély F, Deenick EK, et al. Inherited GINS1 deficiency underlies growth retardation along with neutropenia and NK cell deficiency. *J Clin Invest.* 2017;127(5):1991–2006.
17. Ahmad M, Hameed Y, Khan M, Usman M, Rehman A, Abid U, et al. Up-regulation of GINS1 highlighted a good diagnostic and prognostic potential of survival in three different subtypes of human cancer. *Braz J Biol.* 2021;84:e250575.
18. Fu Q, Zheng H, Wang X, Tang F, Yu H, Wang H, et al. GINS1 promotes the initiation and progression of bladder cancer by activating the AKT/mTOR/c-Myc signaling pathway. *Exp Cell Res.* 2024;440(1):114125.
19. Zhu W, Wu C, Liu Z, Zhao S, Huang J. OTU deubiquitinase, ubiquitin aldehyde binding 2 (OTUB2) modulates the stemness feature, chemoresistance, and epithelial-mesenchymal transition of colon cancer via regulating GINS complex subunit 1 (GINS1) expression. *Cell Commun Signal.* 2024;22(1):420.
20. Liang J, Yao N, Deng B, Li J, Jiang Y, Liu T, et al. GINS1 promotes ZEB1-mediated epithelial-mesenchymal transition and tumor metastasis via β -catenin signaling in hepatocellular carcinoma. *J Cell Physiol.* 2024;239(5):e31237.

21. Ren X, Shen L, Gao S, Transcription Factor. E2F1 enhances hepatocellular carcinoma cell proliferation and stemness by activating GINS1. *J Environ Pathol Toxicol Oncol.* 2024;43(1):79–90.
22. Yang H, Liu X, Zhu X, Zhang M, Wang Y, Ma M, et al. GINS1 promotes the proliferation and migration of glioma cells through USP15-mediated deubiquitination of TOP2A. *iScience.* 2022;25(9):104952.
23. Ge R, Wang C, Liu J, Jiang H, Jiang X, Liu Z. A novel Tumor-Promoting role for nuclear factor IX in glioblastoma is mediated through transcriptional activation of GINS1. *Mol Cancer Res.* 2023;21(3):189–98.
24. Li M, Shi M, Hu C, Chen B, Li S. MALAT1 modulated FOXP3 ubiquitination then affected GINS1 transcription and driven NSCLC proliferation. *Oncogene.* 2021;40(22):3870–84.
25. Li S, Wu L, Zhang H, Liu X, Wang Z, Dong B, et al. GINS1 induced Sorafenib resistance by promoting cancer stem properties in human hepatocellular cancer cells. *Front Cell Dev Biol.* 2021;9:711894.
26. Chen Z, Wang T, Li C, Zhang W, Huang W, Xue J, et al. FOXP1-GINS1 axis promotes DLBCL proliferation and directs doxorubicin resistance. *J Cancer.* 2023;14(12):2289–300.
27. Nusse R. Wnt signaling. *Cold Spring Harb Perspect Biol.* 2012;4(5).
28. Rim EY, Clevers H, Nusse R. The Wnt pathway: from signaling mechanisms to synthetic modulators. *Annu Rev Biochem.* 2022;91:571–98.
29. Fu WB, Wang WE, Zeng CY. Wnt signaling pathways in myocardial infarction and the therapeutic effects of Wnt pathway inhibitors. *Acta Pharmacol Sin.* 2019;40(1):9–12.
30. Russell JO, Monga SP. Wnt/ β -Catenin signaling in liver development, homeostasis, and pathobiology. *Annu Rev Pathol.* 2018;13:351–78.
31. Clevers H, Nusse R. Wnt/ β -catenin signaling and disease. *Cell.* 2012;149(6):1192–205.
32. Liu J, Xiao Q, Xiao J, Niu C, Li Y, Zhang X, et al. Wnt/ β -catenin signalling: function, biological mechanisms, and therapeutic opportunities. *Signal Transduct Target Ther.* 2022;7(1):3.
33. Nusse R, Clevers H. Wnt/ β -Catenin signaling, disease, and emerging therapeutic modalities. *Cell.* 2017;169(6):985–99.
34. Zhou Y, Xu J, Luo H, Meng X, Chen M, Zhu D. Wnt signaling pathway in cancer immunotherapy. *Cancer Lett.* 2022;525:84–96.
35. He S, Tang S. WNT/ β -catenin signaling in the development of liver cancers. *Biomed Pharmacother.* 2020;132:110851.
36. Zhang Y, Wang X. Targeting the Wnt/ β -catenin signaling pathway in cancer. *J Hematol Oncol.* 2020;13(1):165.
37. Cheng X, Xu X, Chen D, Zhao F, Wang W. Therapeutic potential of targeting the Wnt/ β -catenin signaling pathway in colorectal cancer. *Biomed Pharmacother.* 2019;110:473–81.
38. Zhang W, Ruan X, Li Y, Zhi J, Hu L, Hou X, et al. KDM1A promotes thyroid cancer progression and maintains stemness through the Wnt/ β -catenin signaling pathway. *Theranostics.* 2022;12(4):1500–17.
39. Zhao H, Ming T, Tang S, Ren S, Yang H, Liu M, et al. Wnt signaling in colorectal cancer: pathogenic role and therapeutic target. *Mol Cancer.* 2022;21(1):144.
40. Xu X, Pan Y, Zhan L, Sun Y, Chen S, Zhu J, et al. The Wnt/ β -catenin pathway is involved in 2,5-hexanedione-induced ovarian granulosa cell cycle arrest. *Ecotoxicol Environ Saf.* 2023;268:115720.
41. Xue W, Yang L, Chen C, Ashrafizadeh M, Tian Y, Sun R. Wnt/ β -catenin-driven EMT regulation in human cancers. *Cell Mol Life Sci.* 2024;81(1):79.
42. Wang J, Su W, Zhang T, Zhang S, Lei H, Ma F, et al. Aberrant Cyclin D1 splicing in cancer: from molecular mechanism to therapeutic modulation. *Cell Death Dis.* 2023;14(4):244.
43. Cai Z, Wang J, Li Y, Shi Q, Jin L, Li S, et al. Overexpressed Cyclin D1 and CDK4 proteins are responsible for the resistance to CDK4/6 inhibitor in breast cancer that can be reversed by PI3K/mTOR inhibitors. *Sci China Life Sci.* 2023;66(1):94–109.
44. Montalto FI, De Amicis F. Cyclin D1 in cancer: A molecular connection for cell cycle control, adhesion and invasion in tumor and stroma. *Cells.* 2020;9(12).
45. Lee Y, Dominy JE, Choi YJ, Jurczak M, Tolliday N, Camporez JP, et al. Cyclin D1-Cdk4 controls glucose metabolism independently of cell cycle progression. *Nature.* 2014;510(7506):547–51.
46. Semczuk A, Jakowicki JA. Alterations of pRb1-cyclin D1-cdk4/6-p16(INK4A) pathway in endometrial carcinogenesis. *Cancer Lett.* 2004;203(1):1–12.
47. Yu F, Yu C, Li F, Zuo Y, Wang Y, Yao L, et al. Wnt/ β -catenin signaling in cancers and targeted therapies. *Signal Transduct Target Ther.* 2021;6(1):307.
48. Tang W, Hu Y, Tu K, Gong Z, Zhu M, Yang T, et al. Targeting Trop2 by Bruceine D suppresses breast cancer metastasis by blocking Trop2/ β -catenin positive feedback loop. *J Adv Res.* 2024;58:193–210.
49. Kazi A, Xiang S, Yang H, Delitto D, Trevino J, Jiang RHY, et al. GSK3 suppression upregulates β -catenin and c-Myc to abrogate KRas-dependent tumors. *Nat Commun.* 2018;9(1):5154.
50. Wang Y, Xie Y, Dong B, Xue W, Chen S, Mitsuo S, et al. The TTYH3/MK5 positive feedback loop regulates tumor progression via GSK3- β / β -catenin signaling in HCC. *Int J Biol Sci.* 2022;18(10):4053–70.
51. Zhang J, Wang E, Li Q, Peng Y, Jin H, Naseem S, et al. GSK3 regulation Wnt/ β -catenin signaling affects adipogenesis in bovine skeletal muscle fibro/adipogenic progenitors. *Int J Biol Macromol.* 2024;275(Pt 2):133639.

Publisher's note

Springer Nature remains neutral with regard to jurisdictional claims in published maps and institutional affiliations.